Proc. Natl. Acad. Sci. USA
Vol. 95, pp. 6169–6174, May 1998
Cell Biology

Tyrosine kinase-dependent activation of a chloride channel in CD95-induced apoptosis in T lymphocytes

ILDIKÒ SZABÒ*†, ALBRECHT LEPPLE-WIENHUES*, KRISTEN N. KABA*, MARIO ZORATTI‡, ERICH GULBINS*§, AND FLORIAN LANG*†§

*Department of Physiology, University of Tuebingen, Gmelinstrasse 5, 72076 Tuebingen, Germany; and ‡Consiglio Nazionale delle Ricerche Unit for Biomembranes, Department of Biomedical Sciences, University of Padova, Via Colombo 3, 35121 Padova, Italy

Edited by Joseph F. Hoffman, Yale University School of Medicine, New Haven, CT, and approved March 10, 1998 (received for review September 3, 1997)

ABSTRACT **CD95/Fas/APO-1 mediated apoptosis is an important mechanism in the regulation of the immune response. Here, we show that CD95 receptor triggering activates an outwardly rectifying chloride channel (ORCC) in Jurkat T lymphocytes. Ceramide, a lipid metabolite synthesized upon CD95 receptor triggering, also induces activation of ORCC in cell-attached patch clamp experiments. Activation is mediated by Src-like tyrosine kinases, because it is abolished by the tyrosine kinase inhibitor herbimycin A or by genetic deficiency of p56lck. *In vitro* incubation of excised patches with purified p56lck results in activation of ORCC, which is partially reversed upon addition of anti-phosphotyrosine antibody. Inhibition of ORCC by four different drugs correlates with a 30–65% inhibition of apoptosis. Intracellular acidification observed upon CD95 triggering is abolished by inhibition of either ORCC or p56lck. The results suggest that tyrosine kinase-mediated activation of ORCC may play a role in CD95-induced cell death in T lymphocytes.**

Programmed cell death can be induced by various physiological and pathological factors, including Fas/Apo-1/CD95, tumor necrosis factor, ceramide, reactive oxygen species (ROS), and bacterial toxins (1, 2). Signal transduction during CD95-induced apoptosis, which is especially important in the regulation of the peripheral immune response (3), has been studied extensively (1, 4, 5). Ceramide, generated by sphingomyelinases, is released upon CD95 triggering and can induce apoptosis by itself (6). Src-like protein tyrosine kinases are also crucial for CD95-induced apoptosis, because their inhibition (7) or the expression of the tyrosine phosphatase FAP (8) prevent cell death. Further, CD95 triggering activates, among other molecules, members of the caspase family, Jun N-terminal kinases and the small G protein Ras (9). Possible targets of the proteases, kinases, and G proteins participating in the signaling pathway still have to be clarified.

Ion channels have been implied in lymphocyte proliferation (10–12). Little is known about the possible role of ion channels in the complex process of CD95-triggered apoptosis. We recently have shown that CD95 triggering, ceramide, and ROS inhibit the most abundant K^+ channel (Kv1.3) in lymphocytes (13–15). We observed that the activity of an outwardly rectifying chloride channel (ORCC) also is changed upon CD95 receptor stimulation. The presence of ORCC has been described in various cell types, e.g., in epithelial cells, fibroblasts, and lymphocytes (16–20). ORCC in lymphocytes is characterized by a strong outward rectification of the current–voltage (I-V) relation, by a slope conductance of approximately 40 pS (in 150 mM NaCl), by the presence of conductance substates, by high open channel noise, and by a complex kinetic behavior (19, 20). Although the conductance and the kinetic appearance of ORCC may vary slightly from patch to patch (19, 20), the mentioned characteristics distinguish this channel from other T lymphocyte chloride channels, e.g., the maxi-chloride channel, the cystic fibrosis transmembrane regulator (CFTR) channel and the small-conductance, osmotic pressure-triggered channel (21–24). The genes for several different chloride channels have been cloned (25, 26); however, the protein(s) forming ORCC have not yet been identified. ORCC is silent in intact, unstimulated lymphocytes, but it can be activated by membrane excision and prolonged depolarization (19, 20). ORCC has been shown to be activated also by the catalytic subunit of protein kinase A (PKA)/ATP when applied on the cytoplasmic side of excised patches and by a membrane-permeable cAMP analog in cell-attached patches (19). Activation of this channel by PKA/ATP is defective in CF cells (27), suggesting that it may contribute to the abnormal regulation of fluid secretion observed in this disease. The physiological function of ORCC in lymphocytes is still not understood.

In this study we report a mechanism of ORCC activation via tyrosine kinases upon CD95 receptor ligation. The results also suggest a possible involvement of ORCC in CD95-induced apoptosis.

MATERIALS AND METHODS

Materials. Anti-mouse CD95 antibody (M-20) was purchased from Upstate Biotechnology, anti-human CD95 antibody (CH11) was from Immunotech (Westbrook, ME), C6-ceramide and C2-dihydroceramide were from Biomol (Plymouth Meeting, PA), diphenylamine carboxylate (DPC) was from Fluka, indoleacetic acid (IAA) was from Research Biochemicals, and 4,4′-diisothiocyanatostilbene-2,2′-disulfonic acid (DIDS) and glibenclamide were from Sigma. Antiphosphotyrosine 4G10 antibody and p56lck kinase were purchased from Upstate Biotechnology and Annexin V conjugated to fluorescein isothiocyanate (FITC) was from Boehringer Mannheim. The cAMP enzyme immunoassay kit was from Cayman Chemicals (Ann Arbor, MI).

Cell Culture. Jurkat and p56lck-deficient JCaM1.6 cells were obtained from American Type Culture Collection (Manassas, VA) and grown in RPMI 1640 medium as described (9). Cells were passaged every day. Herbimycin A (10 μM; Calbiochem) was added 10 h before any assay.

The publication costs of this article were defrayed in part by page charge payment. This article must therefore be hereby marked "*advertisement*" in accordance with 18 U.S.C. §1734 solely to indicate this fact.

This paper was submitted directly (Track II) to the *Proceedings* office.
Abbreviations: CFTR, cystic fibrosis transmembrane regulator; DIDS, 4,4′-diisothiocyanatostilbene-2,2′-disulfonic acid; DPC, diphenylamine carboxylate; IAA, indoleacetic acid; ORCC, outwardly rectifying chloride channel; PKA, protein kinase A; V_m, membrane potential; FITC, fluorescein isothiocyanate.

†To whom reprint requests should be addressed. e-mail: biomed@bpciv.bio.unipd.it (I.S.); florian.lang@uni-tuebingen.de (F.L.).
§E.G. and F.L. contributed equally to this study and, therefore, share last authorship.

Electrophysiology. Patch clamp experiments (28) were performed in both cell-attached and inside-out excised patch configurations. Both the pipette and the bath solutions contained 150 mM NaCl, 5 mM KCl, 1 mM $MgCl_2$, 2.5 mM $CaCl_2$, 10 mM Hepes, pH 7.4. In some experiments the pipette solution contained 140 mM tetraethylammonium chloride, 2.5 mM $CaCl_2$, 5 mM $MgCl_2$, 10 mM Hepes, pH 7.4. For the determination of bicarbonate permeability the procedure described in ref. 29 was used. The pipette was filled with 130 mM $NaHCO_3$, 15 mM NaCl, 1.3 mM $CaCl_2$, 1.6 mM K_2HPO_4, 0.4 mM KH_2PO_4, and 1 mM $MgCl_2$, pH 7.4. The solution was bubbled with 30% CO_2 until it was used for filling the pipette. The bath solution contained 145 mM NaCl instead of 130 mM $NaHCO_3$. The resistance of the electrodes was 3–7 MOhm. The experiments were performed at 27°C in a 0.4-ml chamber, in which cells were perfused at 25 ml/h either with a control solution or with a solution containing the test substance or antibody. The duration of the experiments varied from patch to patch (from 30 to 85 min). Currents were monitored with an EPC-9 (HEKA Electronics, Lambrecht/Pfalz, Germany) amplifier. Data were recorded at 2 kHz sampling rate, low-pass filtered at 300 Hz, and analyzed with TAC software (Instrutech, Mineola, NY). Eight-second voltage ramps were applied at 60-sec intervals to monitor channel activity. For construction of the I-V curves, current amplitude was measured at various potentials from at least two ramps [the first ramp(s) after channel activation and the last ramp of the experiment] for each experiment. P_o was determined by creating event lists from most of the 8-sec ramp periods for each experiment. Cations leaving the cell correspond to outward current and are reported as upward deflections. Membrane potential (V_m) is reported as intracellular with respect to ground. For cell-attached recordings voltages are expressed relative to the cellular resting potential (-39 ± 6 mV). Leak current was not subtracted. For V_m measurements performed in the whole-cell configuration in current clamp mode, the pipette solution contained 128 mM K/glutamate, 1 mM EGTA, 1 mM $MgCl_2$, 0.22 mM $CaCl_2$, and 10 mM Hepes, pH 7.2; the bath solution was a standard Ringer solution of 145 mM NaCl, 10 mM glucose, 5 mM KCl, 2 mM $CaCl_2$, 1 mM $MgCl_2$, and 10 mM Hepes, pH 7.4. The effect of drugs was determined either by switching the control bath solution to a drug-containing solution to check for acute changes, or by incubating the cells for 7 h in RPMI solution at 37°C in the presence of the drug and then measuring V_m.

Induction and Measurement of Apoptosis. Jurkat T lymphocytes (10^6 per well) were pretreated for 15 min with 100 μM each glibenclamide, IAA, and DIDS, 1 mM DPC, and 10 μM herbimycin A or left untreated, stimulated 4 h with 200 ng/ml anti-human CD95 antibody (incubated at 37°C in a humidified incubator during these periods), stained with FITC-AnnexinV, and analyzed by flow cytometry. The percentage of inhibition of apoptosis was determined by measuring and comparing the area under the curve of the histograms of FITC-fluorescence in the control and inhibitor-treated samples. In a separate series of apoptosis measurements, cells were labeled for 12 h with 2 μCi/ml [^{3}H]thymidine, washed, incubated with inhibitors, and stimulated with anti-*human* CD95. DNA fragmentation was determined in triplicates in three experiments by lysis of the cells in H_2O and filtration through nitrocellulose followed by liquid scintillation counting (9). Because small DNA fragments do not bind to the membrane, the decrease of bound radioactivity is a measurement for cell death.

pH Measurements. Jurkat T lymphocytes were stimulated with 200 ng/ml anti-human CD95 antibody for 3.5 h. Cells were loaded for 30 min with 1 μM 2′,7′,-bis-(2-carboxyethyl)-5-(and-6)carboxyl-fluorescein methyl-ester (Molecular Probes). During these periods the cells were kept in a humidified incubator at 37°C and 5% CO_2. Measurements were performed at room temperature in the absence of added CO_2 after washing of the cells twice in a dye-free medium. For spectrophotometric recording, excitation light with an alternating wavelength of 485 and 440 nm from a monochromator light source (Uhl, Germany) was directed through gray filters (nominal transmission 1%, Oriel, Stamford, CT) and was deflected by a dichroic mirror (FT 515 nm, Omega Optical, Brattleboro, VT) into the objective (×40, Zeiss). The emitted fluorescence was measured at 521 nm (Raman Longpass, Omega) by using a photomultiplier tube (213-IP28A, Seefelder Messtechnik, Germany). Cytosolic pH was calibrated with the high potassium/nigericin technique (30). The fluorescence ratios at 485/440 nm were linear with cytosolic pH between 6.5 and 7.5. In all experiments, to reduce the region from which fluorescence was collected, a plate with a pinhole (diameter, 1.6 mm) was placed in the image plane of the phototube. Data acquisition was executed by using a computer program (IMG 8, Lindemann & Meiser, Germany).

p56lck Assay. The activity of Src kinases was determined by autophosphorylation. The experiments were performed by 15-min incubation of p56lck immunoprecipitates in 25 mM Hepes, pH 7.2/150 mM NaCl/1 mM Na_3VO_4/5 mM DTT/10 mM $MgCl_2$/0.5% Nonidet P-40/10 μM ATP/10 μCi [^{32}P]γATP (3,000 Ci/mmol; DuPont/NEN). Samples were separated by SDS/PAGE and analyzed by autoradiography.

RESULTS

We examined first the biophysical properties of ORCC in inside-out excised patches from untreated Jurkat T lymphocytes. In accordance with previous reports, ORCC was characterized by high open channel noise, by the presence of conductance substates, and by a slope conductance of approximately 40 pS at 0 mV, which varied slightly from patch to patch (19, 20). Fig. 1*A* shows the characteristic, strong, outwardly rectifying open-channel I-V relation of ORCC from control, inside-out excised patches. ORCC activity was never observed in these patches unless the patch was held at +60 to +80 mV for 1–5 min. ORCC was detected in 48% of the excised patches ($n = 134$). Reducing chloride concentration in the bath from 150 to 75 mM shifted the reversal potential in excised patches by -14 ± 2 mV ($n = 3$, not shown). ORCC was observed in excised patches by using a pipette solution containing tetraethylammonium chloride ($n = 6$). Both results indicate chloride selectivity.

To investigate the activity of ORCC upon CD95 ligation, patch clamp experiments in cell-attached configuration were performed on Jurkat cells either stimulated via CD95 or left untreated. In accordance with previous reports (16, 17) ORCC was always silent in the cell-attached configuration under control conditions ($n = 59$), i.e., the probability of the channel being open (P_o) was zero. The presence of ORCC in each patch was tested by subsequent excision and sustained depolarization. Treatment of Jurkat cells with 200 ng/ml monoclonal anti-human CD95 antibody resulted in an increase of the channel's P_o from 0 to 0.59 ± 0.19 (SD) in 9 of 10 cell-attached experiments in which ORCC was present. In 11 further experiments no activation could be observed. The lack of ORCC in these 11 patches was ascertained by subsequent patch excision and depolarization. Thus, 9 successful activations were achieved out of 21 attempts (43%). We monitored the channel activity by applying short voltage ramps from +80 to −80 mV ($-V_{pip}$) and leaving the cells at resting potential between the ramps, to avoid any possible influence of an imposed steady-state voltage on channel activation. Activity before (Fig. 1*B Upper*) and after stimulation (Fig. 1*B Lower*) from the same cell-attached patch is shown in Fig. 1*B*. ORCC was activated within 4.7 ± 1.5 min and remained active for at least 80 min. Polyclonal anti-mouse CD95 antibody (200 ng/ml), which does not bind to human CD95 and was used as

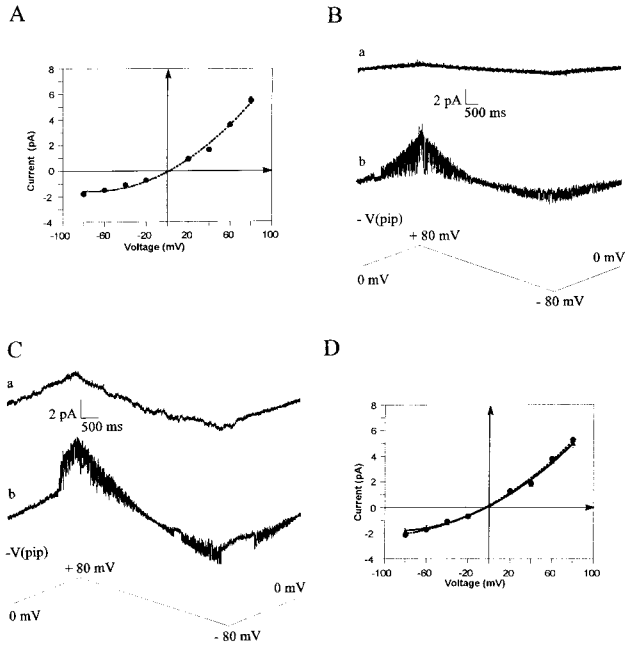

FIG. 1. ORCC is activated by CD95 ligation. (*A*) Open channel I-V relation of ORCC activity in inside-out excised patches in control condition. ORCC was activated by patch excision and depolarization. Error bars represent SEM based on $n \geq 20$ amplitudes measured per potential from 10 different experiments. For every current trace recorded in excised patches voltages are expressed with reference to the pipette solution. (*B*) ORCC activity in cell-attached configuration before (trace a) and after perfusion of the cells with 200 ng/ml anti-human CD95 antibody for 11 min (trace b). Voltage ramps were applied as indicated at 60-sec intervals. For every current trace recorded in on-cell patches voltages are expressed relative to the resting potential. Between the ramps patches were held at resting potential for all cell-attached recordings and at 0 mV for all excised patches. (*C*) Anti-mouse CD95 antibody does not stimulate ORCC in human Jurkat T lymphocytes in the cell-attached patch configuration after 20 min of incubation (trace a). After excision and depolarization ORCC is activated (trace b). (*D*) Open channel I-V curve of channels recorded in cell-attached configuration after stimulation of the cells with 200 ng/ml anti-human CD95 antibody (■) or with 200 μM dibutyryl-cAMP (●). All data are expressed as arithmetic mean ± SEM ($n \geq 14$ for each point, obtained from nine and seven experiments, respectively).

control, failed to activate ORCC in cell-attached patches (Fig. 1*C Upper*), even if ORCC was present in the patch (Fig. 1*C Lower*, $n = 6$). The channel activated by anti-human CD95 antibody displayed typical ORCC activity and chloride selectivity, as assessed by using a pipette solution containing tetraethylammonium chloride ($n = 5$). As shown on Fig. 1*D*, the open channel I-V curves of ORCC recorded from CD95-triggered patches or from control excised patches were not significantly different.

ORCC has been shown to be activated by the cAMP-regulated CFTR (19, 27), which is expressed in human T and B lymphocytes (31, 32). Fig. 1*D* shows the I-V curve of the channels activated by 200 μM dibutyryl-cAMP in cell-attached patches ($n = 7$; in six further experiments ORCC was not present in the patch). The channels activated by CD95 triggering and by dibutyryl-cAMP displayed similar activities. However, in accordance with a recent study (33), in our experiments CD95 ligation failed to change cAMP levels or to stimulate PKA (not shown). This result suggested that activation of ORCC by CD95 triggering was not mediated by cAMP.

To gain some insight into the molecular mechanism of CD95-induced activation of ORCC, we tested whether ceramides mimic the effect of anti-human CD95 antibodies on ORCC. Ceramides have been shown to be important mediators of CD95-induced apoptosis (6, 9, 34), and lymphocytes lacking the acidic sphingomyelinase are resistant to CD95-triggered apoptosis (35). Synthetic C6-ceramide (20 μM), but not the inactive stereoisomer dihydro-C2-ceramide (20 μM, $n = 5$), activated ORCC in cell-attached patches (Fig. 2*A*), indicating a specificity of the effect of C6-ceramide. Incubation

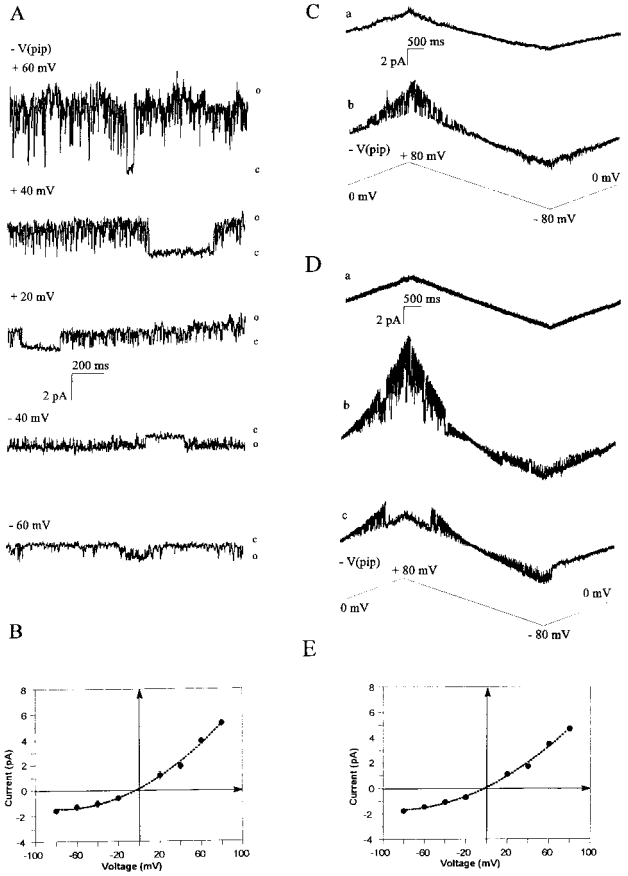

FIG. 2. ORCC is activated by a signaling cascade involving ceramides and Src-like tyrosine kinases. (*A*) Perfusion with C6-ceramide (20 μM) results in activation of ORCC. Shown are representative current traces at steady-state potentials in cell-attached configuration 7 min after C6 ceramide addition. In the experiment shown the open probability of the channel increased from 0 to 0.93 ± 0.4 at 8 different voltages. Traces were selected to show channel closures. The activity upon ceramide treatment did not show significant voltage dependence in most experiments. Open and closed levels are indicated. (*B*) I-V curves of channels activated by 20 M C6-ceramide in cell-attached configuration. All data are expressed as arithmetic mean ± SEM ($n \geq 18$ for each point, obtained from nine different experiments). (*C*) Pretreatment of Jurkat with 10 μM herbimycin A for 10 h prevents ORCC activation upon perfusion with 200 ng/ml anti-human CD95 antibody. Shown is a current trace in cell-attached configuration (trace a) from a herbimycin A-pretreated cell incubated with anti-CD95 for 17 min and a trace (b) from the same patch after patch excision and depolarization demonstrating the presence of ORCC. (*D*) Addition of purified p56lck to excised patches activates ORCC (trace b). Active ORCC is inactivated by the addition of anti-phosphotyrosine antibodies 4G10. Shown is a representative current trace from an inside-out excised patch held at 0 mV before (trace a) and 5 min after the addition of 2 units purified p56lck + 10 μM ATP (trace b). Trace c was recorded from the same patch after perfusion of the patch chamber with 10 μg/ml antiphosphotyrosine antibodies 4G10 (in the presence of p56lck and ATP). Upon addition of p56lck two ORCC were active (b) whereas only one channel remained relatively active after the addition of 4G10 (c) in the same patch. (*E*) Open channel current–voltage relation of ORCC activated by purified p56lck in inside-out excised patches. Error bars represent SEM based on $n \geq 12$ amplitudes measured per potential from six different experiments.

of the cells with C6-ceramide resulted in a significant increase of the P_o from 0 to 0.71 ± 0.24 in 9 of 10 cells. Fig. 2*B* shows the I-V curve of the channels activated in these cells. In seven further experiments ORCC was not present (9 activations of 17 attempts; 53%).

CD95 ligation and ceramide treatment have been shown to stimulate Src-like tyrosine kinases (7, 36, 37). Activation of ORCC was prevented by pretreatment with herbimycin A, an inhibitor of Src-like tyrosine kinases ($n = 6$) (Fig. 2*C*). In accordance with previous reports (7, 37), herbimycin A reduced CD95-induced apoptosis by 80%. In JCaM 1.6 cells, a Jurkat cell clone genetically deficient for p56lck (38), the major Src-like tyrosine kinase in Jurkat cells, anti-human CD95 antibody failed to activate ORCC in all 5 cell-attached patches of the 16 patches in which ORCC was present.

To further study the significance of tyrosine kinase for ORCC activation, inside-out excised patches from Jurkat cells were incubated with 2 units/ml of purified p56lck enzyme plus 10 μM ATP at 0 mV. The addition of p56lck activated ORCC within 5 min and caused an increase of P_o from 0 to 0.68 ± 0.22 ($n = 6$ of 13 trials; in 7 experiments ORCC was not present in the patch) (Fig. 2*D*). The I-V curve of the channels activated by purified p56lck is shown on Fig. 2*E*. In excised control patches held at 0 mV the channel was never activated ($n = 134$) even in the presence of 10 μM ATP ($n = 2$). After activation of ORCC by p56lck, 10 μg/ml anti-phosphotyrosine antibodies 4G10 were added to the cytosolic surface of excised inside-out patches ($n = 3$), resulting in a significant decrease of the P_o from 0.74 ± 0.15 to 0.35 ± 0.21 (two-tailed *t* test; $P < 0.0002$) (Fig. 2*D*). The molar ratio between the added p56lck and the 4G10 was approximately 1:5. An isotype-matched monoclonal mouse Ig had no effect ($n = 2$, not shown). As tested by measuring autophosphorylation of p56lck, its kinase activity was not diminished upon addition of 4G10 antibodies (not shown). We conclude that ORCC activation by CD95 triggering involves ceramides and the tyrosine kinase p56lck.

To study the significance of ORCC activation by CD95, we inhibited the channel and measured the rate of apoptosis. Because the ORCC gene is not cloned, only pharmacological inhibitors, i.e., stilbene derivatives, IAA, DPC, calixarene, and glibenclamide, can be applied (20, 39–42). We first determined the concentrations at which these inhibitors themselves did not affect cell viability. Afterward, we tested the effect of these known inhibitors, at the nontoxic concentrations, on ORCC activity in Jurkat T lymphocytes. In agreement with earlier findings (40), 100 μM glibenclamide caused a 78 ± 9% reduction of the open probability of ORCC in inside-out excised patches held at different potentials ($n = 3$) (Fig. 3*A*). In outside-out patches the block is almost complete (40). IAA (100 μM) ($n = 3$; Fig. 3*B*) and 1 mM DPC ($n = 2$, not shown) inhibited the channel as well, as reported previously (20, 39). Therefore, we used these concentrations of the substances to check the effect of ORCC inhibition on CD95-induced apoptosis.

The inhibition of ORCC by different compounds correlated with a 30–65% reduction of CD95-triggered apoptosis assessed either by flow cytometric analysis of FITC-Annexin binding to the cells (Fig. 3 *C* and *D*) ($n = 6$ for each drug) or, in a separate set of experiments, by DNA fragmentation measurements (Fig. 3*E*) ($n = 9$ for each inhibitor). The Annexin V fluorescence increase upon CD95 triggering was not significant in the early phase of apoptosis (0.5–2 h) whereas changes were evident after 4 h. IAA and glibenclamide were most effective in reducing CD95-induced cell death (Fig. 3 *C–E*). The results obtained by measuring apoptosis with the two methods were in good agreement both for glibenclamide [an inhibition of apoptosis by 65 ± 9% (Annexin binding) and by 53 ± 4% (DNA fragmentation) was observed] and for IAA (48 ± 8% and 55 ± 4% reduction in apoptosis, respectively). DPC (1 mM) and the stilbene derivative DIDS (100 μM) had

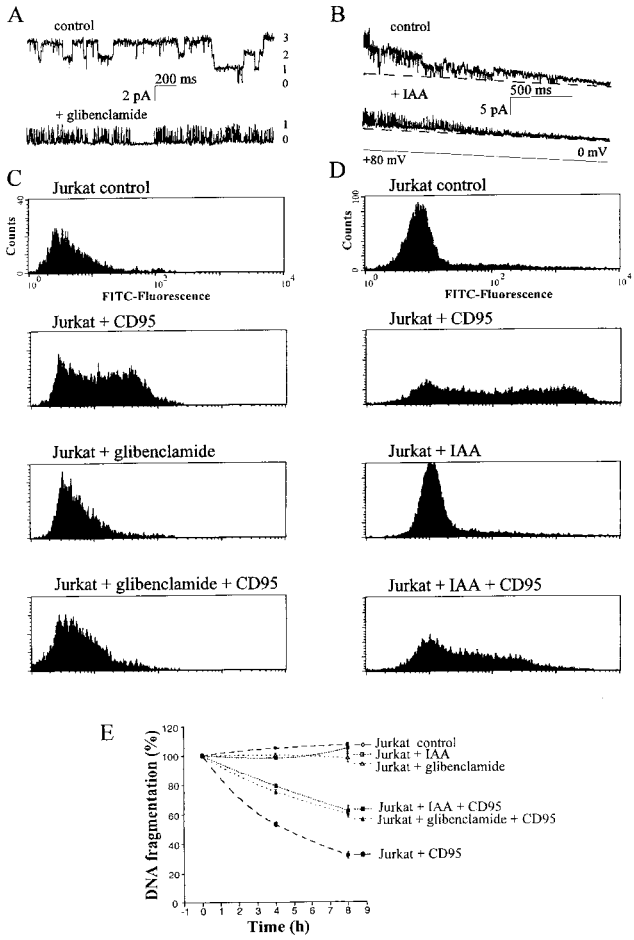

FIG. 3. Glibenclamide and IAA block ORCC and CD95 induced apoptosis. (*A*) Displayed are traces from an inside-out excised patch held at +40 mV in control condition (*Upper*) and 2 min after perfusion of the chamber with 100 μM glibenclamide (*Lower*). The results are representative for three experiments. (*B*) Representative current traces from an inside-out excised patch before (*Upper*) and after 8-min (*Lower*) incubation with 100 μM IAA. Dashed line shows closed level. (*C*) Treatment of Jurkat cells with 100 μM glibenclamide inhibits CD95-triggered apoptosis determined by binding of FITC-Annexin V and fluorescence-activated cell sorter analysis. Cells were incubated for 4 h with 200 ng/ml anti-human CD95 antibody in the presence or absence of glibenclamide. Shown are representative histograms of FITC-fluorescence. Apoptosis was reduced by 63 ± 4% in six independent experiments. (*D*) IAA (100 μM) reduces CD95-triggered apoptosis. Apoptosis was determined as in *C*. Shown are representative histograms of four experiments. (*E*) Treatment of Jurkat cells with 100 μM glibenclamide or 100 μM IAA reduces CD95-triggered apoptosis, measured by fragmentation of [^{3}H]thymidine-labeled DNA. All data are expressed as arithmetic mean ± SEM ($n = 9$ for each point). Differences between CD95-triggered apoptosis in the absence and in the presence of inhibitors are significant at 4 and 8 h of incubation ($P < 0.05$, two-tailed *t* test).

less of an effect (32 ± 7% and 30 ± 4% reduction of apoptosis, respectively; not shown). Higher concentrations of DIDS affected the viability of control cells and therefore could not be used for apoptosis tests. 100 μM DIDS caused a partial, flickering block of the channel in excised patches ($n = 2$, not shown). Because these drugs, in particular glibenclamide, an inhibitor of ABC transporters/channels, might have changed the V_m, we tested whether this was the case. The V_m was −33.1 ± 4.6 mV in control cells, −31.1 ± 5.2 mV upon acute treatment of Jurkat cells with 100 μM glibenclamide ($n = 4$) and −33.8 ± 4.1 mV after 7 h of incubation with the same concentration used ($n = 4$). 5,11,17,23-Tetrasulfonato-

25,26,27,28-tetramethoxy-calix(4)arene (TS-TM calixarene; 300 nM) inhibited neither apoptosis nor ORCC channel activity in on-cell patches in Jurkat cells. The correlation between inhibition of ORCC function and partial inhibition of apoptosis by four different drugs suggests that ORCC may be involved in CD95-induced apoptosis.

CD95-triggered apoptosis in Jurkat cells is preceded by intracellular acidification, and treatment with alkalinizing reagents reduces apoptosis pointing to an important role of cytosolic pH (43). The outwardly rectifying channel may directly conduct bicarbonate in various cells (29, 44) or it may favor, by release of Cl^-, the cellular release of bicarbonate in exchange for Cl^- (on the Cl^-/HCO_3^- exchanger). ORCC of Jurkat cells also is permeable to bicarbonate because application of 130 mM HCO_3^- in the pipette solution resulted in a 21.5 ± 1.5 mV shift of the reversal potential, revealing a permeability ratio $P_{HCO_3^-}/P_{Cl^-}$ of 0.38 ± 0.03 ($n = 4$). Therefore, we investigated a possible role of ORCC activation for CD95-induced acidification. CD95 ligation induced a significant cellular acidification by 0.6 pH units within 4 h, which was strongly inhibited by glibenclamide or IAA (100 μM) (Fig. 4*A*). Furthermore, intracellular acidification was blocked in cells pretreated with herbimycin A or in JCaM1.6 cells (Fig. 4*B*). These data suggest that the p56lck mediated-ORCC activation upon CD95 may result in cellular acidification. However, activation of ORCC during apoptosis may influence other processes, e.g., volume regulation or maintenance of V_m as well.

DISCUSSION

In this report we show activation of an outwardly rectifying chloride channel by CD95 receptor ligation. The data obtained applying pharmacological and genetic methods show that tyrosine phosphorylation of ORCC itself or of a regulatory protein is required for the activation of the channel by CD95 triggering. The results also suggest that ORCC activation is one step in the chain of events leading to apoptosis.

Tyrosine kinases are essential for CD95-induced apoptosis and have multiple cellular target molecules in lymphocytes. The *in vitro* activation of ORCC by p56lck may reflect a direct modification of the channel. However, other molecule(s) present in the patch conceivably could serve as mediator(s) between p56lck and ORCC. The partial reversal of p56lck-induced activation by the anti-phosphotyrosine antibody 4G10 suggests that ORCC or an associated regulatory protein is activated via direct tyrosine phosphorylation. The result of the kinase assay suggests that 4G10 does not inhibit ORCC by direct inhibition of p56lck. The observation that shows inactivation of a channel upon addition of 4G10, suggests that phosphorylated tyrosine residue(s) might play a role in channel gating. We recently have studied activation of chloride channels resembling ORCC by purified p56lck in whole-cell experiments as well (45). Cloning and purification of ORCC will be necessary to determine precisely the phosphorylation target. The P_o of CFTR channels have been shown to increase by tyrosine kinase $p60^{c\text{-}src}$ and the tyrosine phosphatase inhibitor vanadate (46). Therefore, it is possible that activation of ORCC by tyrosine kinases in our experiments was mediated by CFTR, which is expressed at low levels in lymphocytes (32). However, we could not observe activation of the biophysically distinct CFTR chloride channels upon apoptosis triggering.

ORCC is known to be inhibited by various, not highly specific substances. Glibenclamide also inhibits ATP-sensitive K^+ channels, which, however, are not expressed in lymphocytes (47). In accordance, glibenclamide practically did not alter V_m. ORCC and CFTR are the only other reported targets of glibenclamide (40). DPC also inhibits both chloride channels. On the other hand, IAA and DIDS inhibit ORCC, but not CFTR. The inhibitory effect of four different inhibitors of

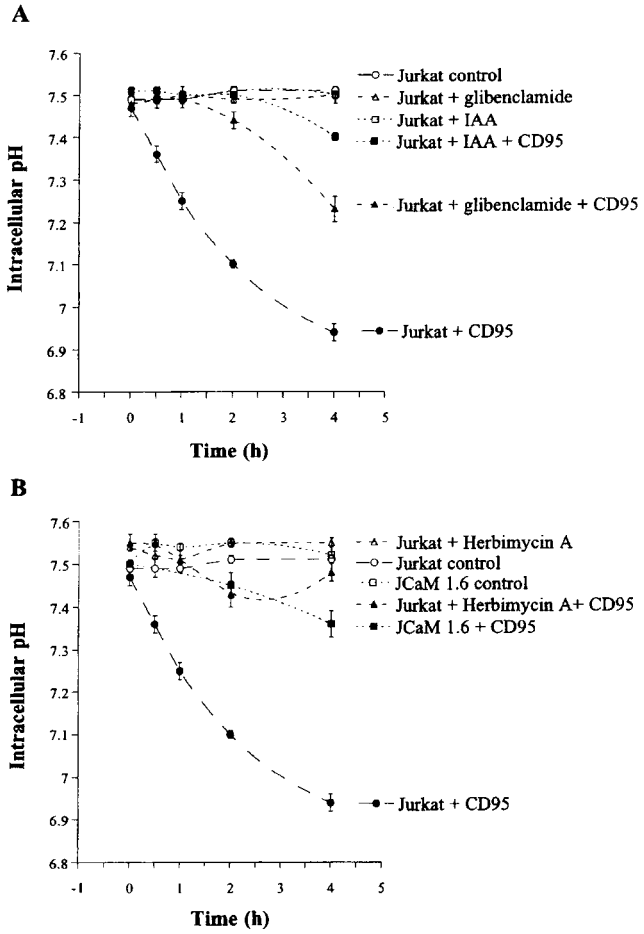

FIG. 4. Cellular acidification upon CD95 stimulation is prevented by glibenclamide and IAA (*A*) or by genetic deficiency or pharmacological inhibition of Src-like tyrosine kinases (*B*). (*A*) Treatment of Jurkat cells with 200 ng/ml anti-human CD95 antibody induces a time-dependent reduction of intracellular pH. Cellular acidification is inhibited by 100 μM glibenclamide or by 100 μM IAA. All data are expressed as arithmetic mean ± SEM ($n = 20–60$ for each point). (*B*) Genetic deficiency of p56lck in JCaM1.6 cells or inhibition of Src-like tyrosine kinases by preincubation with 10 μM herbimycin A for 10 h prevents cellular acidification upon stimulation with 200 ng/ml anti-human CD95. Differences are significant ($P < 0.05$, two-tailed *t* test) 30 min after CD95 triggering. All data are expressed as arithmetic mean ± SEM ($n = 20–60$ for each point).

ORCC on CD95-induced apoptosis suggests the involvement of ORCC in apoptosis. However, we cannot exclude the possibility that another protein, involved in CD95-triggered apoptosis, is inhibited by all four substances. The involvement of ORCC in apoptosis might be confirmed once its gene has been identified. A role for CFTR in cycloheximide-induced apoptosis recently has been suggested in epithelial cells because its inhibition by DPC and a mutation in its gene protected against such a process (48). CFTR, which is expressed in lymphocytes at lower levels than in epithelial cells (31, 32), is insensitive to IAA and DIDS, which inhibited CD95-induced apoptosis. Furthermore, lymphocytes derived from CF patients ($n = 3$) showed normal CD95-induced cell death rates when compared with control lymphocytes (E.G., J.S., F.L., unpublished data).

The physiological function of ORCC in lymphocytes is unknown. Possible roles include maintenance of V_m, macromolecule secretion, and regulation of volume and bicarbonate secretion. Gottlieb *et al.* (43) reported that intracellular acidification to approximately pH 6.8, measured by fluorescence-activated cell sorter analysis, occurs within 3 h upon CD95

triggering in Jurkat T lymphocytes and precedes DNA fragmentation. Treatment of Jurkat cells with various apoptosis-inducing agents also resulted in cellular acidification. Our results, obtained by measuring intracellular pH of individual cells after CD95 stimulation, are in good agreement with this report. The acidic pH possibly activates endonucleases that may be responsible for chromatin digestion during apoptosis. Our results show that inhibitors of ORCC prevent intracellular acidification, suggesting that ORCC may, at least in part, mediate this process, probably by allowing bicarbonate efflux. The findings that CD95 triggering fails to induce acidification in herbimycin A-treated cells and in Jurkat cells deficient of p56lck kinase and that in these cells ORCC was not activated upon CD95 triggering also would favor this hypothesis. However, activation of ORCC during apoptosis also may influence processes other than acidification. Intracellular acidification itself also may exert an effect on V_m. ORCC activation may result in an efflux of bicarbonate, possibly leading to (*i*) an intracellular acidification because of the continuous replenishment of the carbonic acid species by diffusion of CO_2; and (*ii*) a limited decrease of V_m because of the efflux of negative charges. In the absence of CO_2 these processes would be expected to be much more limited in scope and transient. Acidification-induced depolarization has been reported in T lymphocytes (49). In addition, bicarbonate-dependent pH regulation is known to occur and to depend on membrane potential in epithelial cells (50).

In summary, in the present work we show that an outwardly rectifying chloride channel, ORCC, is up-regulated in CD95-induced apoptosis. We provide evidence that activation upon CD95-triggering is mediated by tyrosine phosphorylation, a novel mechanism of ORCC regulation. Our results also suggest an involvement of ORCC in CD95-induced apoptosis, possibly through an effect on intracellular pH.

We thank C. Mueller and P. Barth for technical assistance, Dr. B. Brenner for help with cAMP measurement, and Dr. T. Laun for help with membrane potential measurements. We are grateful to Prof. O. Pongs and Drs. A. Ghazi, H. Apfel, and A. Angrilli for critical reading of the manuscript. TS-TM-calix(4)arene was a kind gift of Dr. Bridges. This work was supported by grants from the Deutsche Forschungsgemeinschaft to F.L. (La315/4–2) and to E.G. (Gu335/2–2, AICR 96–18, and the JKFZ Tuebingen). I.S. is grateful to European Molecular Biology Organization for a long term fellowship.

1. Thompson, C. B. (1995) *Science* **267,** 1456–1462.
2. Nagata, S. & Goldstein, P. (1995) *Science* **267,** 1449–1456.
3. Singer, G. G. & Abbas, A. K. (1994) *Immunity* **1,** 365–372.
4. Gulbins, E., Szabò, I. & Lang, F. (1996) *Cell. Physiol. Biochem.* **6,** 361–375.
5. Nagata, S. (1997) *Cell* **88,** 355–365.
6. Hannun, Y. A. (1996) *Science* **274,** 1855–1859.
7. Eischen, C. M., Dick, C. J. & Leibson, P. J. (1994) *J. Immunol.* **153,** 1947–1954.
8. Sato, T., Irie, S., Kitada, S. & Reed, J. C. (1995) *Science* **268,** 411–415.
9. Gulbins, E., Bissonette, R., Mahboubi, A., Nishioka, W., Brunner, T., Baier, G., Baier-Bitterlich, G., Byrd, C., Lang, F., Kolesnik, R., *et al.* (1995) *Immunity* **2,** 341–351.
10. Chandy, K. G., DeCoursey, T. E., Cahalan, M. D., McLaughlin, C. & Gupta, S. (1984) *J. Exp. Med.* **160,** 369–376.
11. Lewis, R. S. & Cahalan, M. D. (1990) *Annu. Rev. Physiol.* **52,** 415–428.
12. Phipps, D. J., Branch, D. R. & Schlichter, L. C. (1996) *Cell Signal* **8,** 141–149.
13. Szabo, I., Gulbins, E., Apfel, H., Zhang, X., Barth, P., Busch, A. E., Schlottmann, K., Pongs, O. & Lang, F. (1996) *J. Biol. Chem.* **271,** 20465–20469.
14. Gulbins, E., Szabo, I, Baltzer, K, & Lang, F. (1997) *Proc. Natl. Acad. Sci. USA* **94,** 7661–7666.
15. Szabo, I., Nilius, B., Zhang, X., Busch, A. E., Gulbins, E., Suessbrich, H. & Lang, F. (1997) *Eur. J. Physiol. Pflügers Arch.* **433,** 626–632.
16. Schoumacher, R. A., Shoemaker, R. I., Halm, D. R., Tallant, E. A., Wallace, R. W. & Frizzell, R. A. (1987) *Nature (London)* **330,** 752–754.
17. Li, M., McCann, J. D., Liedtke, C. M., Nairn, A. C., Greeangard, P. & Welsh, M. J. (1988) *Nature (London)* **331,** 358–360.
18. Bear, C. E. (1988) *FEBS Lett.* **237,** 145–149.
19. Chen, J. H., Schulman, H. & Gardner, P. (1989) *Science* **243,** 657–660.
20. Garber, S. S. (1992) *J. Membr. Biol.* **127,** 49–56.
21. Gallin, E. K. (1991) *Physiol. Rev.* **71,** 775–804.
22. Nishimoto, I., Wagner, J. A., Schulman, H. & Gardner, P. (1991) *Neuron* **6,** 547–555.
23. Lewis, R. S., Ross, P. E. & Cahalan, M. D. (1993) *J. Gen. Physiol.* **101,** 801–826.
24. Pahapill, P. A. & Schlichter, L. C. (1992) *J. Membr. Biol.* **125,** 171–183.
25. Thiemann, A., Grunder, S., Pusch, M. & Jentsch, T. J. (1992) *Nature (London)* **356,** 57–60.
26. Paulmichl, M., Li, Y., Wickman, K., Ackerman, M., Peralta, E. & Clapham, D. (1992) *Nature (London)* **356,** 238–241.
27. Egan, M., Flotte, T., Afione, S., Solow, R., Zeitlin, P. L., Carter, B. J. & Guggino, W. B. (1992) *Nature (London)* **358,** 581–583.
28. Hamill, O. P., Marty, A., Neher, E., Sakmann, B. & Sigworth, F. J. (1981) *Eur. J. Physiol. Pflügers Arch.* **391,** 85–100.
29. Kunzelmann, K., Gerlach, L., Froebe, U. & Greger, R. (1991) *Eur. J. Physiol. Pflügers Arch.* **417,** 616–621.
30. Thomas, J. A., Buchsbaum, R. N., Zimniak, A. & Racker, E. (1979) *Biochemistry* **18,** 2210–2218.
31. McDonald, T. V., Nghiem, P. T., Gardner, P. & Martens, C. L. (1992) *J. Biol. Chem.* **267,** 3242–3248.
32. Krauss, R. D., Bubien, J. K., Drumm, M. L., Zheng, T., Peiper, S. C., Collins, F. S., Kirk, K. L., Frizzell, R. A. & Rado, T. (1992) *EMBO J.* **11,** 875–883.
33. Anderson, K. L., Anderson, G., Michell, R. H., Jenkinson, E. J. & Owen, J. T. (1996) *J. Immunol.* **156,** 4083–4091.
34. Cifone, M. G., DeMaria, R., Roncali, P., Rippo, M. R., Azuma, M., Lainer, L. L., Santoni, A. & Testi, R. (1994) *J. Exp. Med.* **180,** 1547–1552.
35. Woodle, E. S., Smith, D. M., Bluestone, J. A., Kirkman, W. M., Green, D. R. & Skowronski, E. W. (1997) *J. Immunol.* **158,** 2156–2164.
36. Ji, L., Zhang, G. & Hirabayashi, Y. (1995) *Biochem. Biophys. Res. Commun.* **215,** 489–496.
37. Schlottmann, K. E., Gulbins, E., Lau, S. M. & Coggeshall, K. M. (1996) *J. Leukocyte Biol.* **60,** 546–554.
38. Straus, D. B. & Weiss, A. (1992) *Cell* **70,** 585–593.
39. Cliff, W. H., Schoumacher, R. A. & Frizzell, R. A. (1992) *Am. J. Physiol.* **262,** C1154–C1160.
40. Rabe, A., Disser, J. & Frömter, E. (1995) *Eur. J. Physiol. Pflügers Arch.* **429,** 659–662.
41. Schwiebert, E. M., Egan, M. E., Hwang, T. H., Fulmer, S. B., Allen, S. S., Cutting, G. R. & Guggino, W. B. (1995) *Cell* **81,** 1063–1073.
42. Singh, A. K., Venglarik, C. J. & Bridges, R. J. (1995) *Kidney Int.* **48,** 985–993.
43. Gottlieb, R. A., Nordberg, J., Skowronski, E. & Babior, B. M. (1996) *Proc. Natl. Acad. Sci. USA* **93,** 654–658.
44. Tabcharani, J. A., Jensen, T. J., Riordan, J. R. & Hanrahan, J. W. (1989) *J. Membr. Biol.* **112,** 109–122.
45. Lepple-Wienhues, A., Szabo, I., Laun, T., Kaba, N. K., Gulbins, E. & Lang, F. (1998) *J. Cell Biol.*, **141,** 281–286.
46. Fischer, H. & Machen, T. E. (1996) *Biophys. J.* **71,** 3073–3082.
47. Mix, E., Zhu, J., Olsson, T. & Link, H. (1994) *Autoimmunity* **18,** 233–241.
48. Gottlieb, R. A. & Dosanjh, A. (1996) *Proc. Natl. Acad. Sci. USA* **93,** 3587–3591.
49. Mason M. J. & Grinstein, S. (1990) *J. Membr. Biol.* **116,** 139–148.
50. Poulsen, J. H. & Machen, T. E. (1996) *Eur. J. Physiol. Pflügers Arch.* **432,** 546–554.